Multifragmentation in $E/A = 35$ MeV Collisions: Evidence for a Coulomb Driven Breakup?

M. D'Agostino,[2] G. J. Kunde,[6] P. M. Milazzo,[2] J. D. Dinius,[6] M. Bruno,[2] N. Colonna,[1] M. L. Fiandri,[2] C. K. Gelbke,[6] T. Glasmacher,[6] F. Gramegna,[3] D. O. Handzy,[6] W. C. Hsi,[6] M. Huang ,[6] M. A. Lisa,[6,*] W. G. Lynch,[6] P. F. Mastinu,[2] C. P. Montoya,[6,†] A. Moroni,[4] G. F. Peaslee,[6,‡] L. Phair,[6,*] R. Rui,[5] C. Schwarz,[6,§] M. B. Tsang,[6] G. Vannini,[5] and C. Williams[6]

[1]*INFN, Via Amendola 173, 70126 Bari, Italy*
[2]*Dipartimento di Fisica and INFN, Via Irnerio 46, 40126 Bologna,Italy*
[3]*INFN, Laboratori Nazionali di Legnaro, Via Romea 4, 35020 Legnaro, Italy*
[4]*INFN, Via Celoria 12, 20133 Milano, Italy*
[5]*Dipartimento di Fisica and INFN, Via Valerio 2, 34127 Trieste,Italy*
[6]*National Superconducting Cyclotron Laboratory and Department of Physics and Astronomy, Michigan State University, East Lansing, Michigan 48824*

(Received 3 May 1995)

Multifragment disintegrations have been measured for central Au+Au collisions at $E/A = 35$ MeV. Fragment emission occurs predominantly at low center of mass energies of about $E/A \approx 5$ MeV, consistent with a Coulomb dominated breakup of a single source. Mean fragment multiplicities of $\langle N_{\mathrm{IMF}} \rangle \approx 10.8$ are extracted after correction for the detection efficiency. The fragment charge distributions decrease much more gradually than expected from scaling laws recently applied to the extraction of critical exponents for the nuclear liquid-gas phase transition from nuclear collisions.

PACS numbers: 25.70.Pq, 25.70.Gh

Very highly charged nuclear systems are fundamentally unstable. At low excitation energies this instability manifests itself by the binary fission of heavy ($Z > 90$) nuclei [1], and at higher excitation energies, by the binary disintegration of highly charged systems ($184 \geq Z \geq 92$) formed momentarily in central, near Coulomb barrier collisions [2]. Coulomb [3] and isospin effects [4] are also predicted to strongly modify the characteristics of low density phase transitions in nuclear matter and to significantly alter the collision dynamics, increasing the likelihood of a multifragment disintegration [5–8]. The predicted consequences of Coulomb instabilities include the formation of bubblelike multifragment breakup configurations in central collisions at $E_{\mathrm{beam}}/A \approx 30$ MeV [8], and a flattening of the fragment charge distributions with decreasing excitation energy [5,6]. If true, this latter prediction could invalidate present techniques for the extraction of critical exponents from fragment charge distributions [9–11] and complicate [6] the extrapolation of present measurements to the limit of infinite nuclear matter.

Even though the Coulomb interaction is known to strongly modify nuclear properties, little is experimentally known about Coulomb driven multifragment decays. Collisions between highly charged Au nuclei at incident energies of $E/A = 100$ MeV, are characterized by a very large collective expansion of the compressed central region formed during the early stages of the collision [12,13]. For such violent collisions, Coulomb instabilities may play only a minor role. A few measurements of the multifragment disintegration of very highly charged systems ($Z_{\mathrm{tot}} \geq 130$) have been performed at low incident energies ($E/A \approx 30$ MeV), which suggest that bulk multifragmentation processes contribute little to a total reaction cross section dominated by strongly damped binary collisions [14,15]. In this Letter, we present measurements of very central Au+Au collisions at a slightly higher energy, $E/A = 35$ MeV which strongly suggest a Coulomb driven multifragment decay. Consistent with recent molecular dynamics calculations for highly charged systems [5], we observe remarkably flat elemental distributions that are predicted to be a consequence of the destabilizing long range Coulomb interaction and are, therefore, inconsistent with the assumptions underlying recent extractions of critical exponents for the nuclear liquid-gas phase transition [9–11].

The experiment was performed at the National Superconducting Cyclotron Laboratory of Michigan State University. Beams of Au ions at $E/A = 35$ MeV incident energy, accelerated by the K1200 cyclotron, were used to bombard Au foils of approximately 5 mg/cm^2 areal density. Light charged particles and intermediate mass fragments (IMF's: $3 \leq Z_{\mathrm{IMF}} \leq 20$) were detected at $23^\circ \leq \Theta_{\mathrm{lab}} \leq 160^\circ$ by 158 phoswich detector elements of the MSU Miniball [16], and fragments with $3 \leq Z \leq 79$ at $3^\circ \leq \Theta_{\mathrm{lab}} \leq 23^\circ$ by 44 gas-Si-Si(Li)-CsI detectors of the INFN Multics Array [17]. The charge identification thresholds were about 2, 3, and 4 MeV/nucleon in the Miniball for Z = 3, 10, and 18, respectively, and about 1.5 MeV/nucleon in the Multics Array independent of fragment charge. To achieve higher precision in the Miniball energy calibrations, however, a higher energy threshold at laboratory energies of $E/A = 5$ MeV was imposed upon the analysis of particles detected in the Miniball. The geometric acceptance of the combined array was greater than 87% of 4π.

For the analysis reported here, impact parameters were selected via constraints upon the total charged–particle multiplicity detected in the combined system. Assuming that the charged-particle multiplicity decreases monotonically with impact parameter, a "reduced" impact parameter, $\hat{b} = b/b_{\max}$, for each event was determined according to [18]

$$\hat{b} = \frac{b}{b_{\max}} = \left[\int_{N_C(b)}^{\infty} dN_C P(N_C)\right]^{1/2}. \qquad (1)$$

Here, $P(N_C)$ is the probability distribution for the charged-particle multiplicity for $N_C > 2$, and $\pi b_{\max}^2$ is the cross section for collisions with $N_C > 2$.

The analysis focused upon central events with $N_C \geq 28$ corresponding to $\hat{b} \leq 0.1$. For such events, approximately 53% of the total charge is detected in the experimental apparatus, and a surprisingly large fraction, 58%, of this detected charge is bound in intermediate mass fragments, defined here by $3 \leq Z_{\mathrm{IMF}} \leq 20$. Using the inherent symmetry of the Au+Au reaction [19], the detection efficiency was determined and an efficiency corrected mean IMF multiplicity $\langle N_{\mathrm{IMF}} \rangle = 10.8 \pm 1$ was obtained. The corresponding efficiency corrected charge distribution, shown by the solid points in Fig. 1, is surprisingly flat. A similarly flat charge distribution, shown by the open points, is also observed for fragments emitted at center of mass angles of $\theta_{\mathrm{c.m.}} = 90° \pm 20°$, suggesting that the large abundance of heavier fragments does not originate from the decay of projectilelike and targetlike remnants. (Differences between the two sets of data are comparable to the systematic uncertainties in the efficiency correction.) For comparison, we show the charge distribution measured for central collisions at $E/A = 100$ MeV (solid squares) for the same system [20], and the charge distribution measured in peripheral collisions at $E/A = 1000$ MeV for the same system (open squares) [20]. Both of these charge distributions measured at higher energies decrease much more steeply with fragment charge.

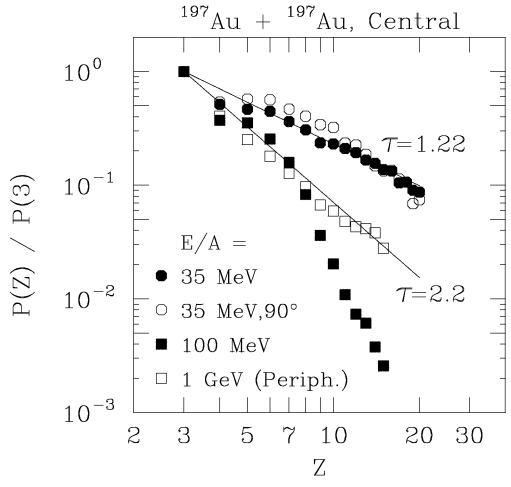

FIG. 1. Efficiency corrected relative elemental probability distribution $P(Z)/P(3)$ for fragments emitted in central collisions ($\hat{b} \leq 0.1$) for the reaction Au+Au at $E/A = 35$ MeV (solid points). The corresponding differential distribution at $\Theta_{\mathrm{c.m.}} = 90° \pm 20°$ is shown as open points. Relative elemental yields for central collisions at $E/A = 100$ MeV and peripheral collisions at $E/A = 1000$ MeV from Ref. [20] are shown by the solid and open squares, respectively.

Early investigations of high-energy hadron-nucleus collisions revealed a power-law behavior, $p(A) \propto A^{-\tau}$, of the inclusive mass distributions [21], similar to that observed for the distributions of droplets for near-critical, macroscopic systems exhibiting a liquid and a gaseous phase [22]. Consistent with this macroscopic analogy, values for the "critical parameter" of τ have been extracted [9,10] from analyses of charge distributions measured for smaller systems containing 80–200 nucleons. After correction for finite size effects and detection efficiency, values for $\tau \approx 2.2$ are obtained for peripheral collisions in the domain of limiting fragmentation; one such example is provided by the data for slowly expanding systems produced via peripheral collisions at $E/A = 1000$ MeV shown in Fig. 1. Similar data have been interpreted [9–11] as evidence for near critical behavior.

Such attempts to extract critical exponents [9–11] from scaling laws have relied heavily upon the assumption that the charge or mass distributions of systems at thermal equilibrium display minimum values for τ at the critical point. The charge distribution in Fig. 1 for $E/A = 35$ MeV can be described in the range of $3 \leq Z \leq 20$ by a χ^2 fit of a power law with values for τ of $\tau = 1.22 \pm 0.05$. This value is much smaller than the value $\tau \approx 2.2$ expected from scaling laws at the critical point of the liquid gas phase diagram. Compared to this difference, finite size corrections to τ, deduced from percolation model calculations for systems with $A \approx 400$ [10], are negligible. This prompts more detailed consideration of other factors that could enhance the production of heavier fragments.

Angular momentum [23,24], Coulomb interactions [3,25], nonequilibrium effects [26], and noncompact decay configurations [27] have been raised previously as important issues but have not been taken into account during the extraction [9–11] of critical exponents. Before focusing upon Coulomb effects, it is worthwhile considering some of these other possibilities. For example, the selection of events with impact parameters $\hat{b} \leq 0.1$ used in the construction of Fig. 1 could include contributions from strongly damped reactions, due to the finite resolution of the impact parameter filter. The importance of the statistical decay of rapidly rotating projectilelike and targetlike residues with enhanced branching ratios for fragment emission [23,24,28] can be assessed by examining the fragment velocity distributions.

Typical examples of such velocity distributions are shown in Fig. 2 for $Z = 7$ and peripheral ($\hat{b} \geq 0.7$, upper panel) and central collisions ($\hat{b} \leq 0.1$, lower panel), respectively [19]. Ringlike emission patterns, centered about the projectilelike and targetlike residue velocities

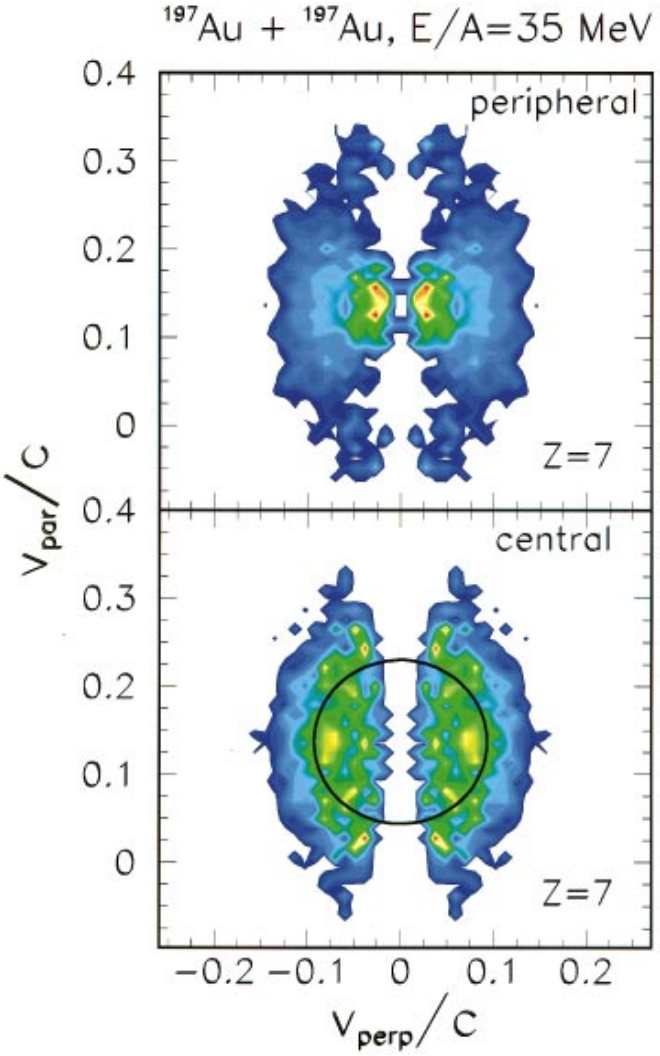

FIG. 2 (color). Velocity distribution $d^2P/v_\perp dv_\parallel dv_\perp$ for $Z = 7$ fragments emitted in peripheral collisions ($\hat{b} \geq 0.7$, upper panel) and central collisions ($\hat{b} \leq 0.1$, lower panel). The velocity axes are in units of the speed of light, and the intensity scale is linear. The circle corresponds to a fixed velocity of $0.1c$ in the center of mass. (In this figure, the efficiency corrected velocity distributions at $v \geq v_{\text{c.m.}}$ have been reflected about the center of mass velocity $v_{\text{c.m.}}$ to obtain a thresholdless distribution for all velocities.)

and characteristic of the statistical decay of rapidly rotating projectilelike and targetlike residues, are only weakly observed. Instead, distributions of IMF's for peripheral and central collisions have a major component centered about the center of mass velocity $v_{\text{c.m.}}$. Fragments are formed primarily in peripheral collisions by the fragmentation of a "neck" that momentarily connects projectilelike and targetlike residues, consistent with previous observations [29]. This "neck" or "overlap region" forms a "participant" source that grows in size and importance with decreasing impact parameter until it encompasses the entire system.

The circle in Fig. 2 corresponds to a constant rms fragment velocity of $v_{\text{rms}} = (\langle v^2_{\text{c.m.}} \rangle)^{1/2} \approx 0.1c$, consistent with the velocity distribution for fragments emitted in central collisions at $70° \leq \Theta_{\text{c.m.}} \leq 110°$ and approximately correct for the participant source at other angles [30]. Such a low value for v_{rms} is roughly consistent with the Coulomb disintegration of a single spherical source at a constant density of about $0.25 - 0.3\rho_0$. This conclusion is supported by the observations in such central Au+Au collisions [30] of fragment c.m. velocities, fragment-fragment correlation functions, and event shape analyses that are consistent with the Coulomb expansion of a spherical source. While these latter results suggest modest angular momentum effects, a precise estimate of such effects is difficult at present, and some angular momentum dependent enhancements [23,24,28] in the branching ratios for noncompound fragment emission may be possible if the decay mechanism is phase space dominated.

Unusually flat fragment charge distributions have been predicted by a number of theoretical investigations. Reduced values of the extracted "effective" critical parameter $\tau \approx 1.7$ have been attributed to the existence of a nonequilibrium mixture of fragments and a supersaturated nucleonic gas at freezeout [9]. Within microcanonical fragmentation models [3,25], the Coulomb interaction causes significantly larger fragment multiplicities [3] and a preference for bubblelike fragment spatial distributions [25]. Within bond percolation models [27], such noncompact bubblelike decay configurations can display values for the critical parameter τ that are 20% smaller than those for compact spherical systems. Classical molecular dynamical simulations of neutral, initially thermalized liquid drops predict a nonequilibrium fragmentation within the region of adiabatic instability [7,26] and for a specific choice of the molecular interaction [26], a reduction in the effective critical exponent τ in heavy systems to minimum values of about $\tau \approx 1.6$. A qualitative change in the dependence of charge distributions upon excitation energy is predicted within molecular dynamics calculations when the Coulomb interaction is introduced [5]. In the calculations of Ref. [5], for example, the calculated slope parameter τ displays a minimum of about $\tau \approx 2.2$ for a neutral system of 394 nucleons at an intermediate temperature of $T_0 = 4-5$ MeV and larger values of τ corresponding to steeper charge distributions at either higher or lower temperatures. With the inclusion of the Coulomb interaction, this minimum disappears and the calculated values for τ decrease monotonically with decreasing temperature to attain $\tau \approx 1.3$ at the lowest calculated temperature, $T \approx 0.2T_0$. While the specific values for τ or temperature may depend upon computational details, the results of Ref. [5] do suggest that the most compelling cause for the extreme flatness of the measured charge distribution is the destabilizing Coulomb interaction. This interpretation is also consistent with the differences between the present measurements

and the measured trends observed for the multifragmentation of less highly charged systems [10,11].

In summary, multifragment disintegrations have been measured for central Au+Au collisions at $E/A = 35$ MeV. Fragment emission occurs predominantly at low emission energies of about $E/A \approx 5$ MeV in the center of mass, consistent with a Coulomb dominated breakup of a single source. Mean intermediate mass fragment multiplicities of $\langle N_{\mathrm{IMF}} \rangle \approx 10.8$ are extracted. Fragment charge distributions are observed that decrease much more gradually than would be consistent with recent extractions of critical exponents for the nuclear liquid-gas phase transition. These observations are qualitatively consistent with trends predicted for Coulomb driven multifragment decays of highly charged systems. Additional experimental and theoretical work is required to quantitatively understand the present observations.

This work was supported by the National Science Foundation under Grant No. Phy-92-14992. The authors are indebted to Professor I. Iori for stimulating and constructive discussions, and to P. Buttazzo, L. Celano, A. Ferrero, L. Manduci, G. V. Margagliotti, F. Petruzzelli, and R. Scardaoni for the help during the measurements. The technical assistance of R. Bassini, C. Boiano, S. Brambilla, G. Busacchi, A. Cortesi, and M. Malatesta is gratefully acknowledged. One of us (G. J. K.) acknowledges the support from the Alexander von-Humboldt Foundation.

*Present address: Nuclear Science Division, Lawrence Berkeley Laboratory, Univ. of California, Berkeley, CA 94720.

†Present address: Merrill Lynch, World Financial Center, North Tower, New York, NY 10281.

‡Present address: Physics Department, Hope College, Holland, MI 49423.

§Present address: Gesellschaft für Schwerionenforschung, D-64220 Darmstadt, Germany.

[1] Robert Vandenbosch and John R. Huizenga, *Nuclear Fission* (Academic Press, New York, 1973), and references therein.

[2] W. U. Schröder and J. R. Huizenga, *Treatise on Heavy Ion Science* (Plenum Press, New York, 1984), Vol. 2, and references therein.

[3] D. H. E Gross *et al.*, Nucl. Phys. **A545**, 187c (1992).

[4] H. Mueller *et al.*, Indiana University Report No. NTC 95-04, 1995 (to be published).

[5] S. Das Gupta and J. Pan, McGill University Preprint McGill/95-27, submitted to Phys. Rev. C (1995).

[6] G. J. Kunde *et al.* (to be published).

[7] A. Vincentini *et al.*, Phys. Rev. C **31**, 1783 (1985); R. J. Lenk *et al.*, Phys. Rev. C **34**, 177 (1986); T. J. Schlagel *et al.*, Phys. Rev. C **36**, 162 (1986).

[8] B. Borderie *et al.*, Phys. Lett. B **302**, 15 (1993).

[9] M. Mahi *et al.*, Phys. Rev. Lett. **60**, 1936 (1988).

[10] T. Li *et al.*, Phys. Rev. Lett. **70**, 1924 (1993).

[11] M. L. Gilkes *et al.*, Phys. Rev. Lett. **73**, 590 (1994).

[12] S. G. Jeong *et al.*, Phys. Rev. Lett. **72**, 3468 (1994).

[13] W. C. Hsi *et al.*, Phys. Rev. Lett. **73**, 3367 (1994).

[14] J. F. Lecolley *et al.*, Phys. Lett. B **325**, 317 (1994).

[15] B. M. Quednau *et al.*, Phys. Lett. B **309**, 10 (1993).

[16] R. T. de Souza *et al.*, Nucl. Instrum. Methods Phys Res., Sect. A **295**, 109 (1990).

[17] I. Iori *et al.*, Nucl. Instrum. Methods Phys. Res., Sect. A **325**, 458 (1993).

[18] C. Cavata *et al.*, Phys. Rev. C **42**, 1760 (1990); Y. D. Kim *et al.*, Phys. Rev. C **45**, 338 (1992).

[19] The detection efficiency $\varepsilon(\theta)$ could be accurately determined at $v \geq v_{\mathrm{c.m.}}$ and $\theta_{\mathrm{lab}} > 3°$. Both the efficiency corrected fragment yield and the efficiency corrected velocity distribution in Fig. 2 were therefore determined at $v \geq v_{\mathrm{c.m.}}$ and reflected about $v = v_{\mathrm{c.m.}}$ to obtain the values for $v \leq v_{\mathrm{c.m.}}$.

[20] G. J. Kunde *et al.*, Phys. Rev. Lett. **74**, 38 (1995).

[21] A. S. Hirsch *et al.*, Phys. Rev. C **29**, 508 (1984).

[22] M. E. Fisher, Physics (Long Island City, N.Y.) **3**, 255 (1967).

[23] W. A. Friedman *et al.*, Nucl. Phys. **A471**, 327c (1987).

[24] L. G. Sobotka *et al.*, Nucl. Phys. **A471**, 111c (1987).

[25] D. H. E Gross *et al.*, Nucl. Phys. **A567**, 317 (1994).

[26] S. Pratt *et al.*, Phys. Lett. B **349**, 261 (1995).

[27] L. Phair *et al.*, Phys. Lett. B **314**, 271 (1995).

[28] K. Sneppen *et al.*, Nucl. Phys. **A480**, 342 (1988).

[29] C. P. Montoya *et al.*, Phys. Rev. Lett. **73**, 3070 (1994).

[30] M. D'Agostino *et al.* (to be published).